 CMES, vol.5, no.3, pp.189-200, 2004

Determination of Stress Intensity Factors for Interfacial Cracks Using the Virtual Crack Extension Approach

W.M.G.. So[1], K.J. Lau[1], S.W. Ng[1]

Abstract: A new finite element analysis procedure is implemented for the determination of complex stress intensity factors in interfacial cracks. Only nodal displacements and strain energies of the near-crack-tip elements are involved in this procedure so that element stiffness matrices need not be made available. The method is first tested using a closed form solution for infinite media to obtain a suitable finite element mesh. It is then applied to finite plates and four-point bending specimens containing interfacial cracks. In cases where reference values are available for comparison, good agreement of results can be obtained with relatively coarse element meshes.

keyword: Fracture, interfacial, cracks, stiffness derivative

1 Introduction

The problems concerning a crack at the interface of two dissimilar materials are gaining importance for their applications in the use of advanced and composite materials, and in electronic packaging. Since the pioneer work of Williams (1959), analytical solutions for such problems remain few and mathematically complicated in their implementations. Summaries of significant advancement can be found in Hutchinson and Suo (1992) and Atluri (1997). The analysis of interfacial cracks in less idealized geometrical configurations and under more general loading conditions is usually obtained through numerical methods. Most of these procedures involve the use of finite element analysis, together with special postprocessing routines, e.g. Lin and Mar (1976), Matos, McMeeking, Charalambides and Drory (1989), Naik and Crews Jr. (1994), Wu (1994), Chow and Atluri (1995), Chow, Beom and Atluri (1995, 1996), Charalambides and Zhang (1996), Glaessgen, Riddell and Raju (2002). Good accuracy has been demonstrated for each procedure. Among these methods Matos, McMeeking, Charalambides and Drory (1989) suggested a method based on evaluation of the J-integral by the virtual crack extension method before and after the perturbation by small increments of the stress intensity factors K_1 and K_2. This approach can be implemented in a relatively straightforward manner but accuracy depends somewhat on the magnitude of the perturbation used. Wu (1994) modified the procedure to remove this dependence. However, in both methods, element stiffness matrices have to be extracted and their derivatives with respect to crack length evaluated for postprocessing purposes. Since commercial finite element codes usually do not include such matrices as standard outputs, special routines have to be written to select the elements involved and to reconstruct such matrices. Ng and Lau (2000) has proposed a new method for finding such derivatives for determining traditional stress intensity factors K_I and K_{II} in isotropic materials. Only nodal displacements and strain energies of the crack-tip elements are needed in the procedure. Since these are standard outputs in most finite element codes, the incorporation of this approach will remove this final barrier for the implementation of the virtual crack extension approach. In this paper the method is extended and combined with the ΔK perturbation approach for the determination of the complex stress intensity factors for interfacial cracks in isotropic media. Suggestions are also made to follow the line of Charalambides and Zhang (1996) and Chow and Atluri (1995) to extend the procedure for applications to orthotropic and anisotropic bimaterial continua.

2 A Virtual Crack Extension Procedure

In the consideration of cracks at bimaterial interfaces (Fig.1), the situation is vastly different from that of cracks in isotropic media. Even when a simple direct load is applied perpendicular to the interface, mixed-mode deformations result for the interface crack. This makes K_I and K_{II} generally indeterminable in the clas-

[1] Dept. of ME, HKPolyU, Hong Kong, China

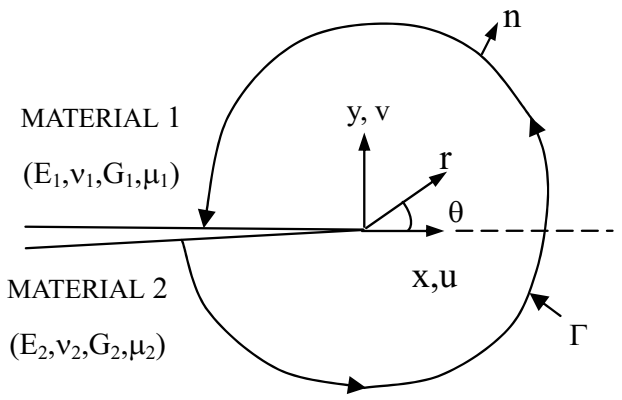

Figure 1: Coordinates and typical contour used to evaluate the J-integral

sical way and standard tests for generating critical K-values as geometry-independent material properties quite impossible. Instead, a complex stress intensity factor, $K = K_1 + iK_2$, is used to characterize the crack tip stresses, with K_1 relating to the effect of a remotely applied direct stress and K_2 relating to that of a remotely applied shear stress. K_1 and K_2, however, neither carry the same physical meaning nor have the same units as K_I and K_{II}. In fact the tensile and shear effects as characterized by this complex stress intensity factor is considered as intrinsically inseparable into analogues of classical modes I and II conditions.

Using the format adopted by Matos et al. (1989), stresses at distance r ahead of the crack tip are given in terms of K_1 and K_2 as:

$$\sigma_{yy} + i\sigma_{xy} = (K_1 + iK_2)\; r^{i\varepsilon} \Big/ \sqrt{2\pi r} \tag{1}$$

$$\text{where} \quad \varepsilon = \frac{1}{2\pi} \ln\left[(\mu_1 G_2 + G_1)/(\mu_2 G_1 + G_2)\right] \tag{2}$$

$i = \sqrt{-1}$ and μ_j equals $(3-\nu_j)/(1+\nu_j)$ in plane stress and equals $3-4\nu_j$ in plane strain. The J-integral is then given by

$$J = \frac{1}{H}\left(K_1^2 + K_2^2\right) \tag{3}$$

where

$$\frac{1}{H} = \frac{1}{2}\left(\frac{1}{E_1'} + \frac{1}{E_2'}\right) \Big/ \cosh^2(\pi\varepsilon) \tag{4}$$

E_j' equals E_j in plane stress and equals $E_j/(1-\nu_j^2)$ in plane strain.

The asymptotic crack tip displacements for the case of $K_2 = 0$ and $K_1 = \Delta K_1$ are given by

$$\Delta u_{x1}^j = \frac{\Delta K_1}{2G_j}\sqrt{\frac{r}{2\pi}}\frac{e^{\pi\varepsilon}}{1+e^{2\pi\varepsilon}} f_{x1}(r,\theta,\varepsilon,\mu_j),$$

$$\Delta u_{y1}^j = \frac{\Delta K_1}{2G_j}\sqrt{\frac{r}{2\pi}}\frac{e^{\pi\varepsilon}}{1+e^{2\pi\varepsilon}} f_{y1}(r,\theta,\varepsilon,\mu_j) \tag{5}$$

Similarly, displacements for the case of $K_1 = 0$ and $K_2 = \Delta K_2$ are:

$$\Delta u_{x2}^j = \frac{\Delta K_2}{2G_j}\sqrt{\frac{r}{2\pi}}\frac{e^{\pi\varepsilon}}{1+e^{2\pi\varepsilon}} f_{x2}(r,\theta,\varepsilon,\mu_j),$$

$$\Delta u_{y2}^j = \frac{\Delta K_2}{2G_j}\sqrt{\frac{r}{2\pi}}\frac{e^{\pi\varepsilon}}{1+e^{2\pi\varepsilon}} f_{y2}(r,\theta,\varepsilon,\mu_j) \tag{6}$$

The functions f are given in the Appendix.

Parks (1974) introduced a stiffness-derivative finite-element technique for determining J by comparing the energy of two slightly different crack lengths so that

$$J = -\left(\partial U/\partial a\right)_F = -\tfrac{1}{2}\{u_n\}^T\left(\partial[S]/\partial a\right)\{u_n\} \tag{7}$$

where U is the potential energy of the body and the differentiation with respect to crack length a is carried out at fixed load F. [S] is the stiffness matrix. Using the virtual crack extension technique only elements connected to the crack-tip are involved so that the stiffness derivative can be evaluated by forward difference as:

$$\frac{\partial\left[S_k^{ct}\right]}{\partial a} = \frac{1}{\Delta a}\left(\left[S_k^{ct}\right]_{a+\Delta a} - \left[S_k^{ct}\right]_a\right) \tag{8}$$

where Δa denotes the magnitude of the infinitesimal crack extension (Figure 2) and $\left[S_k^{ct}\right]_a$, $\left[S_k^{ct}\right]_{a+\Delta a}$ are the element stiffness matrices of crack tip elements with and without the infinitesimal crack extension respectively.

Originally, Parks (1974) suggested extracting the element stiffness matrices in order to evaluate the partial derivative on the right hand side of Eq. 8. Unfortunately, the

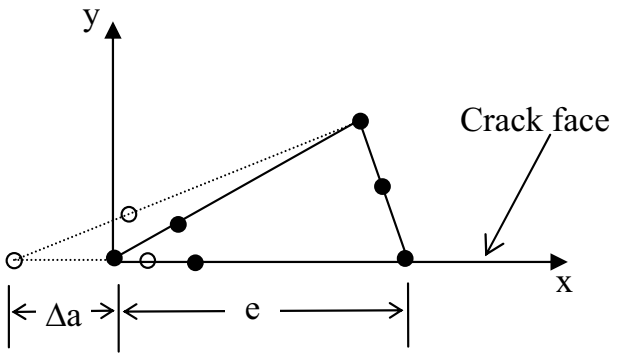

Figure 2 : Crack tip extension

required extraction function is usually not readily available in commercial finite element packages. Substituting Eq. 8 into Eq. 7 and then expanding we obtain

$$J = \frac{1}{\Delta a}\left(\frac{1}{2}\sum_{k=1}^{N_1}\left\{u_k^{ct}\right\}^T\left[S_k^{ct}\right]_a\left\{u_k^{ct}\right\} - \frac{1}{2}\sum_{k=1}^{N_1}\left\{u_k^{ct}\right\}^T\left[S_k^{ct}\right]_{a+\Delta a}\left\{u_k^{ct}\right\}\right) \quad (9)$$

The first term in the bracket of Eq. 9 can be viewed as the total strain energy of the crack tip elements without the crack extension. The second term can be regarded as the total strain energy of the crack tip elements with the crack extension *when subjected to a nodal displacement vector loading which is identical to the previous vector solution without the crack extension.* Since the strain energy of individual element can be either obtained directly using the specific command of commercial finite element packages or generated from stress and strain outputs, the calculation of the first term does not cause any difficulty. The second term can be obtained as follows: firstly, the original problem without crack extension is solved with finite element analysis; secondly, a finite element analysis is performed on a problem in which the nodal displacement solutions without crack extension are imposed as prescribed boundary conditions on the corresponding nodes of the crack tip elements with crack extension. Then, the required second term can be found by summing up the individual strain energy of the crack tip elements with crack extension. Since only the crack-tip elements are perturbed during crack extension process (Figure 2), the finite element mesh for evaluating the second term consists of the crack-tip elements only. Eq. 9 can be rewritten as:

$$J = \frac{1}{\Delta a}\left(U_a^{ct} - U_{a+\Delta a}^{ct}\right) \quad (10)$$

The above procedure can be generalized so that other rings of elements around the crack-tip can be chosen as the perturbed elements for stiffness derivative evaluations. In the present case, in order to avoid the singularities that would be encountered by displacement increment calculations on the crack-tip elements, the second ring of elements, i.e. the transition elements, are chosen. The virtual crack extension is introduced by movement of all the crack-tip element nodes for a distance of Δa in the direction of the crack extension. In this way only transition elements are perturbed while the crack-tip elements will only undergo rigid body movements and hence not contributing to the stiffness derivative. The integrated procedure for determining K_1 and K_2 are then as follows:

Firstly finite element analysis and subsequent virtual crack extension are performed on the system for which the stress intensity factors are to be determined, resulting in, from Eqs. 3 and 10,

$$\frac{K_1^2 + K_2^2}{H} = \frac{1}{\Delta a}\left(U_a^{ct} - U_{a+\Delta a}^{ct}\right)_{u_n} = A \quad (11)$$

Secondly, we choose an arbitrary value of ΔK_1 and superimpose the corresponding displacements $\Delta u_1=(\Delta u_{x1},\Delta u_{y1})$ from Eq. 5 onto u_n to be used as nodal boundary conditions for finite element and virtual crack extension procedures on the transition elements, resulting in

$$\frac{(K_1+\Delta K_1)^2 + K_2^2}{H} = \frac{1}{\Delta a}\left(U_a^{ct} - U_{a+\Delta a}^{ct}\right)_{u_n+\Delta u_1} = B \quad (12)$$

ΔK_1 is related to Δu_1 through equation (4).

In the procedure of Wu (1994), the related equations are:

$$\frac{K_1^2 + K_2^2}{H} = -\tfrac{1}{2}\left\{u_n\right\}^T\left(\partial[S]/\partial a\right)\left\{u_n\right\} = A \quad (13)$$

$$\frac{(K_1+\Delta K_1)^2 + K_2^2}{H} = -\tfrac{1}{2}\left\{u_n+\Delta u_1\right\}^T\left(\partial[S]/\partial a\right)\left\{u_n+\Delta u_1\right\} = B \quad (14)$$

$$\frac{\Delta K_1^2}{H} = -\tfrac{1}{2}\{\Delta u_1\}^T \left(\partial[S]/\partial a\right)\{\Delta u_1\} = C \tag{15}$$

Subtracting Eqs. 13 and 15 from Eq. 14 gives

$$K_1 = -\frac{H}{2\Delta K_1}\{\Delta u_1\}^T \left(\partial[S]/\partial a\right)\{u_n\}$$

$$= \frac{H}{2\Delta K_1}(B-A-C) \tag{16}$$

As explained in Wu (1994) since ΔK_1 is proportional to Δu_1, the result is independent of the choice ΔK_1. Hence K_1 can now be determined with A and B from Eqs.11 and 12 and with C from the chosen ΔK_1value. A similar operation will give the value of K_2, or alternatively, K_2 can be found by back-substituting the K_1 result into either Eq. 11 or Eq. 12.

3 Test cases

3.1 Interface crack in an infinite dissimilar material under biaxial loading (Fig. 3)

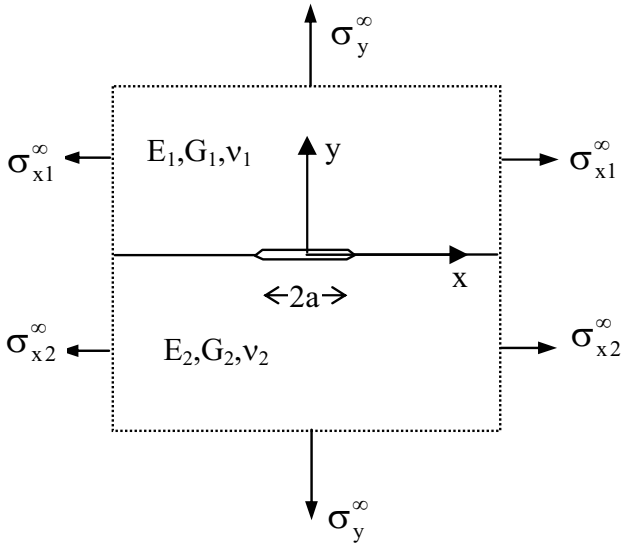

Figure 3: Biaxially loaded crack

From Murakami (1987), the stress intensity factor is given by

$$K_1 + iK_2 = \sigma_y^\infty (1+2i\varepsilon)\sqrt{\pi a}\,(2a)^{-i\varepsilon} \tag{17}$$

while σ_x^∞ is defined as

$$\sigma_{x2}^\infty = \frac{1}{1+\mu_2}\left[\frac{G_2}{G_1}(1+\mu_1)\sigma_{x1}^\infty + \left\{3-\mu_2-\frac{G_2}{G_1}(3-\mu_1)\sigma_y^\infty\right\}\right]$$

but does not affect the stress intensity factors.

The closed form solution for this case is used to establish the appropriate finite element mesh for the analysis of interfacial cracks. Quarter-point crack-tip elements are employed in the analysis to account for stress singularity. In the case of isotropic materials, the recommended size (e) of the crack-tip element is about a/50 and the virtual crack extension (Δa) ranges between 10^{-5} and 10^{-3} of the crack-tip element size. A focused mesh at the crack-tip with gradual enlargement of element size according to a geometric progression scheme is usually employed. Each of these three arrangements are investigated in turn, using E_1/E_2 = 100, $\nu_1 = \nu_2$ = 0.3, $\sigma_y^\infty = \sigma_{x1}^\infty$= 1, and a finite width plate model with crack length to plate-width ratio of 1/10. The reference value from Eq. 17 are K_1 = 1.79874 and K_2 = -0.262529. A typical element mesh is illustrated in Fig. 4. To ensure the circular crack-tip and circular transition elements to progress smoothly into rectangular elements, the elements at the crack-tip are specially formed as shown in Fig. 5. On the crack line the three elements on either side of the crack-tip are given the same length of side, e, while elements beyond are enlarged progressively using a factor equal to m.

Firstly, keeping Δa to 10^{-3} of e, and a moderate adjacent element-size ratio (m) of 1.5, the value of e is varied over a large range of values. The K-values determined using the above method are shown in Fig. 6. It can be seen that the K-values obtained are quite insensitive to element size. . High accuracy can be achieved with very coarse element meshes. For e/a $<$ 1/50, errors are below 0.4% and 0.5% for K_1 and K_2 respectively.

Secondly, keeping e = a/100, m is varied from 1.2 to 4 for e/a = 1/4, 1/10 and 1/100. The results are given in Fig. 7a and Fig.7b. It can be seen that K_2 values are affected more as m is increased. For m $\leq$ 2.5, K-values are very stable. Errors are around 0.4% and 0.5% for K_1 and K_2 respectively.

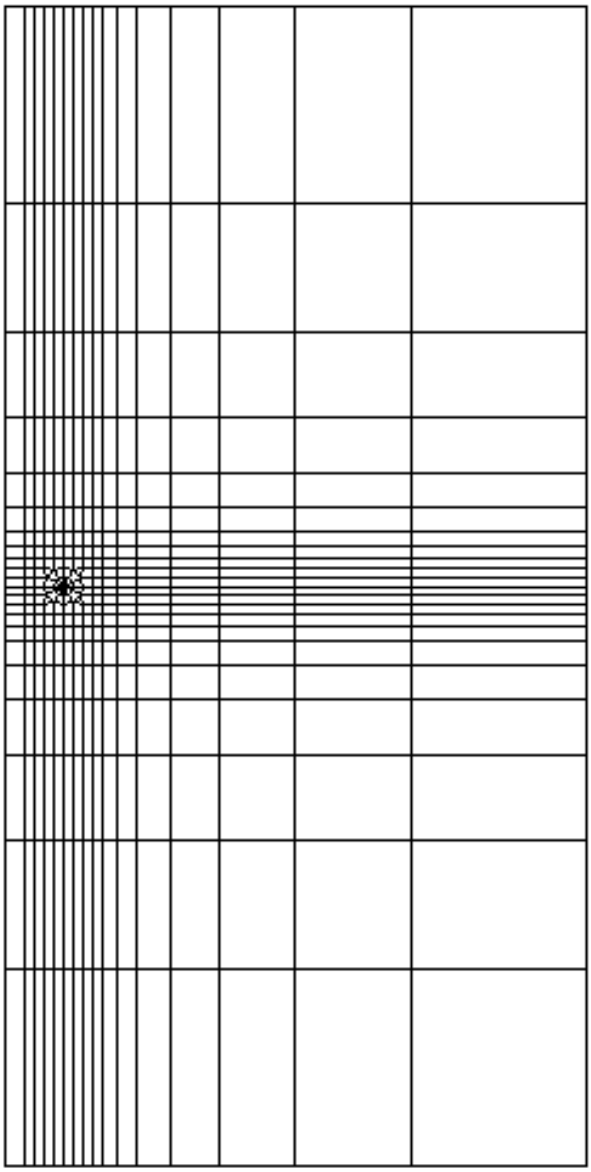

Figure 4 : Half Plate with m = 1.5 , e/a = 1/6

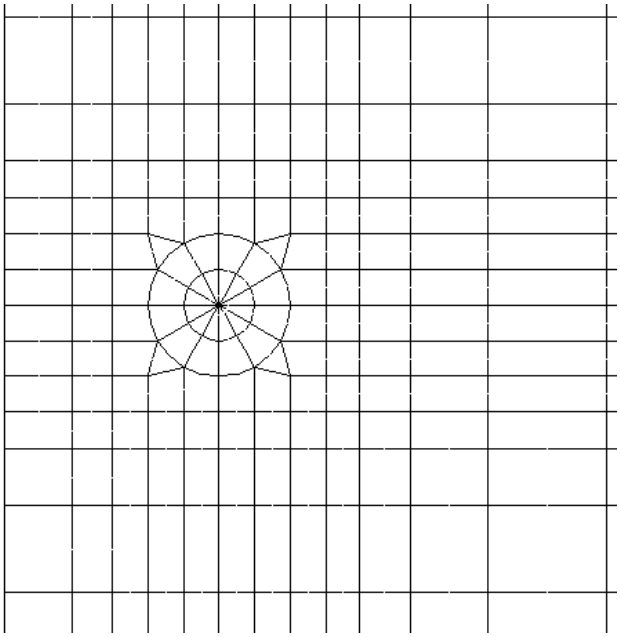

Figure 5 : Crack-tip mesh

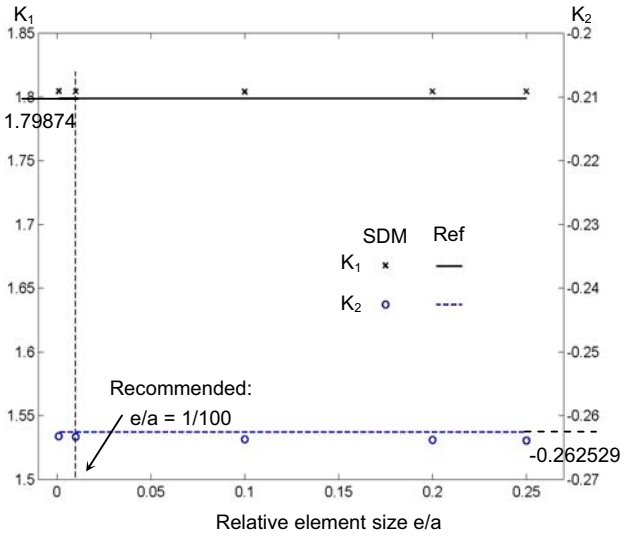

Figure 6: Effect of relative element size e/a on K values– remote biaxial load

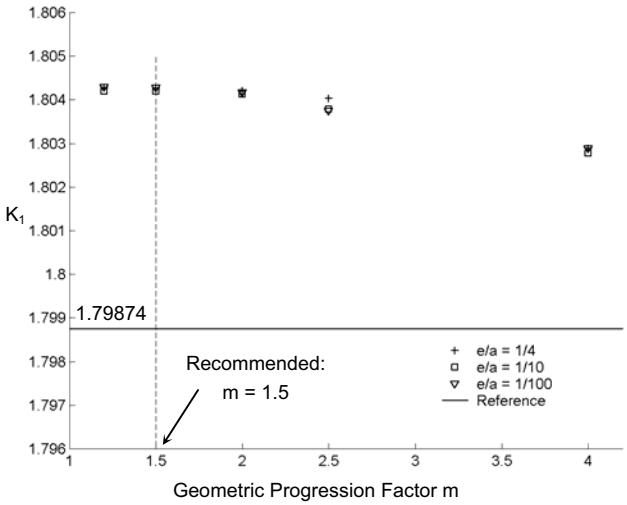

Figure 7a: Effect of geometric progression factor m coupled with element size e/a on K_1 – remote biaxial load

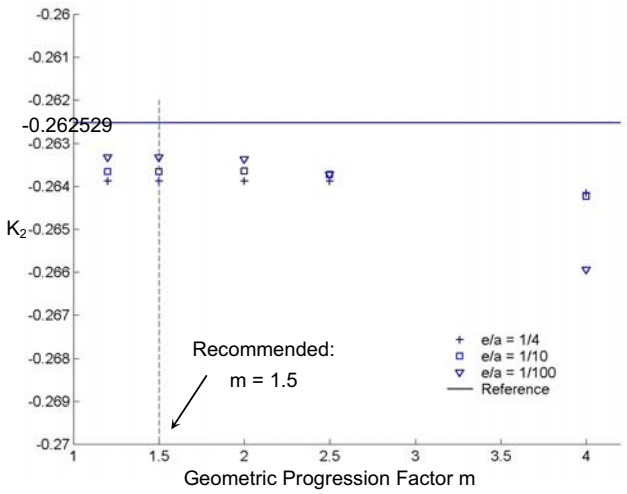

Figure 7b: Effect of geometric progression factor m coupled with element size e/a on K_2 – remote biaxial load

It should be noted that by redesigning the element mesh in areas away from the crack tip, numbers of elements used could have been considerably reduced in the majority of cases, especially cases with small e-values. Since computing time and hardware requirements are not critical in the present study, taking into account the range of element size and number involved, an optimal mesh is not actively pursued. Suffice to say that the present method can be confidently implemented with a relatively coarse mesh and moderate m-values.

To consider the effect of virtual crack extension size, an infinite plate with central crack is analyzed, with e/a = 100, m = 1.5 and a total of 1132 elements. The reference values for K_I and K_{II} are 1.798740 and -0.262529 respectively. The results are shown in Fig.8. Basing on these results it is recommended that Δa/e should be about 1/500 to 1/1000 to ensure that deviations are below 0.5%.

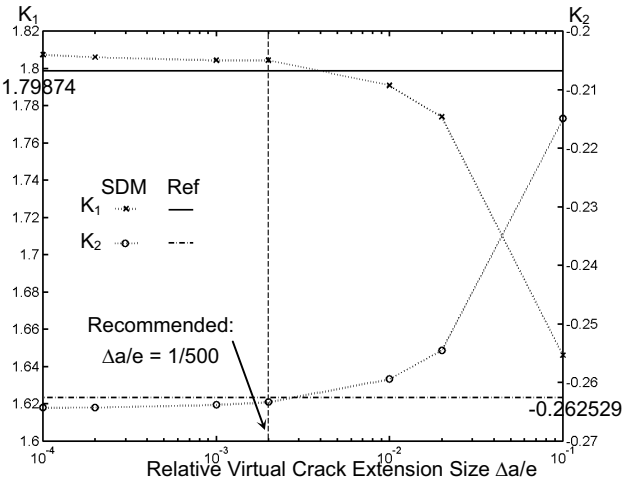

Figure 8: Effect of relative virtual crack extension Δa/e on K values – remote biaxial load

3.2 Central interface crack in a finite bi-material plate under uniform tension (Fig. 9)

By symmetry, only half of the plate needs to be analyzed. Plane stress conditions are applied with: i) symmetry along the plane of symmetry, ii) $u_y = 0$ on the bottom edge and iii) $\sigma = 1$ along the top edge. Fig. 10a-c below show the results with e/a=1/100, m = 1.5, and Δa/e = 1/500. References values are derived from those of Yuuki and Cho as reported in Murakami (1987). A phase angle shift has to be applied since the definition for the complex

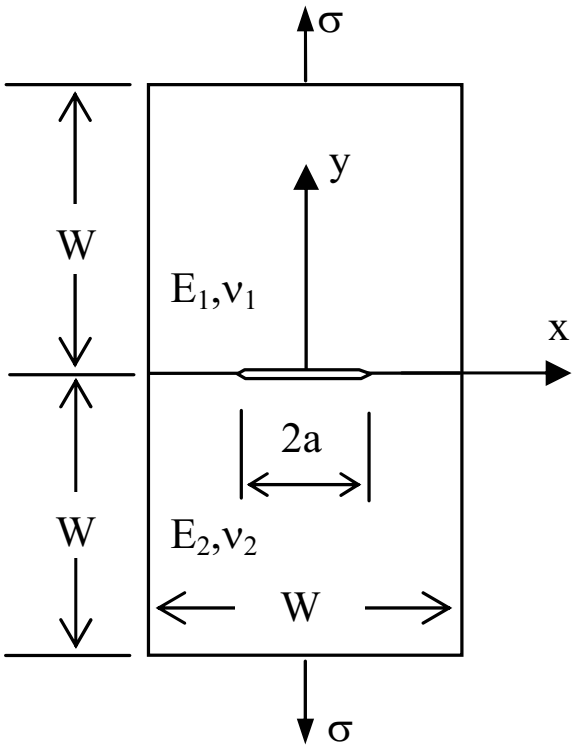

Figure 9 : Central interface crack

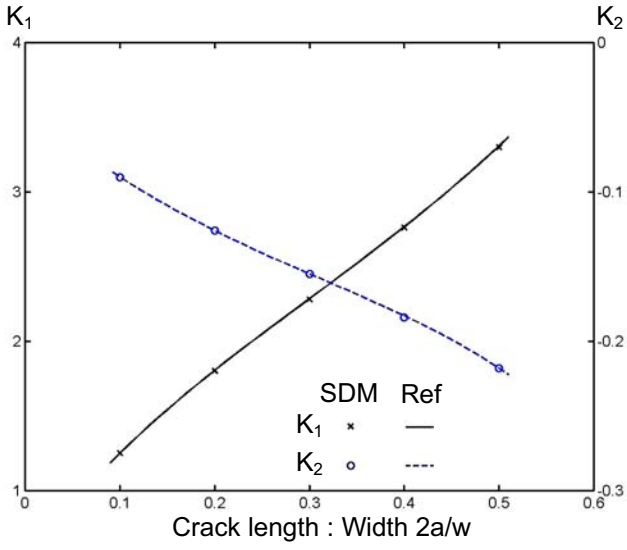

Figure 10a: K values for different 2a/W– central crack in finite plate (with $E_1/E_2 = 2$)

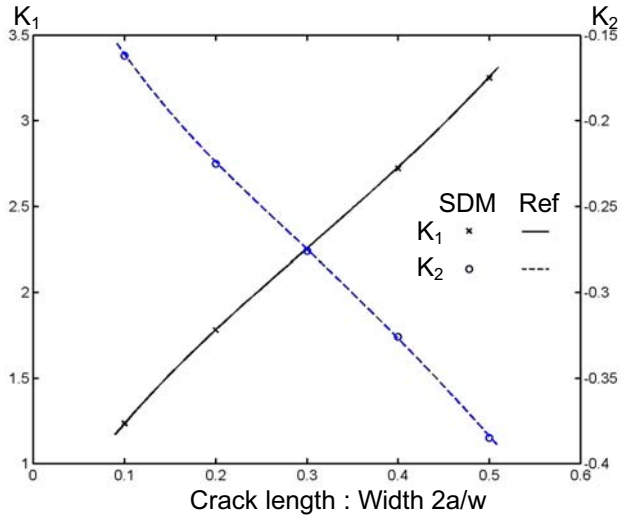

Figure 10b: K values for different 2a/W – central crack in finite plate (with $E_1/E_2 = 4$)

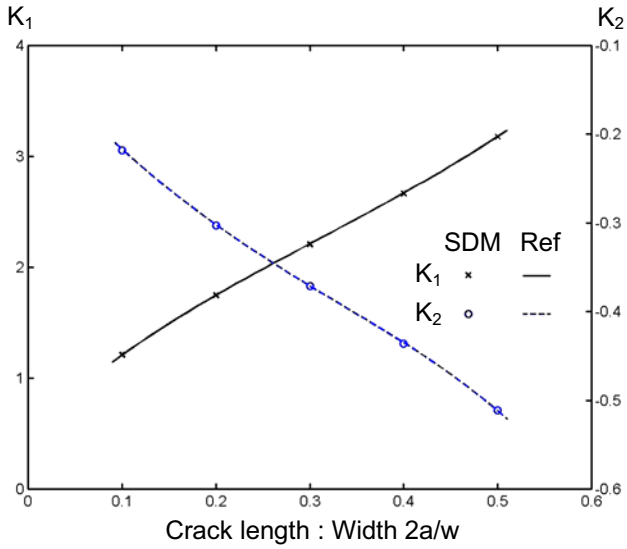

Figure 10c: K values for different 2a/W – central crack in finite plate (with $E_1/E_2 = 10$)

stress intensity factors includes a normalization factor of $(2a)^{-i\varepsilon}$. The maximum deviation is around 0.6%.

3.3 Single edge interface crack in a finite bi-material plate under uniform tension (Fig.11)

With e/a=1/100, m =1.5, Δa/e = 1/500, and σ = 1, different combinations of a/W (crack length : plate width) and E_1/E_2 (modulus ratio) are modeled. Reference values are again derived from those of Yuuki and Cho as reported in Murakami (1987). Fig.12a-c shows the results of having bottom edge fixed u_y=0 and with the remote corner u_x=0, and with pressure σ = 1 on the upper edge. Deviations from reference values are generally rather small, being less than 0.5% in most cases.

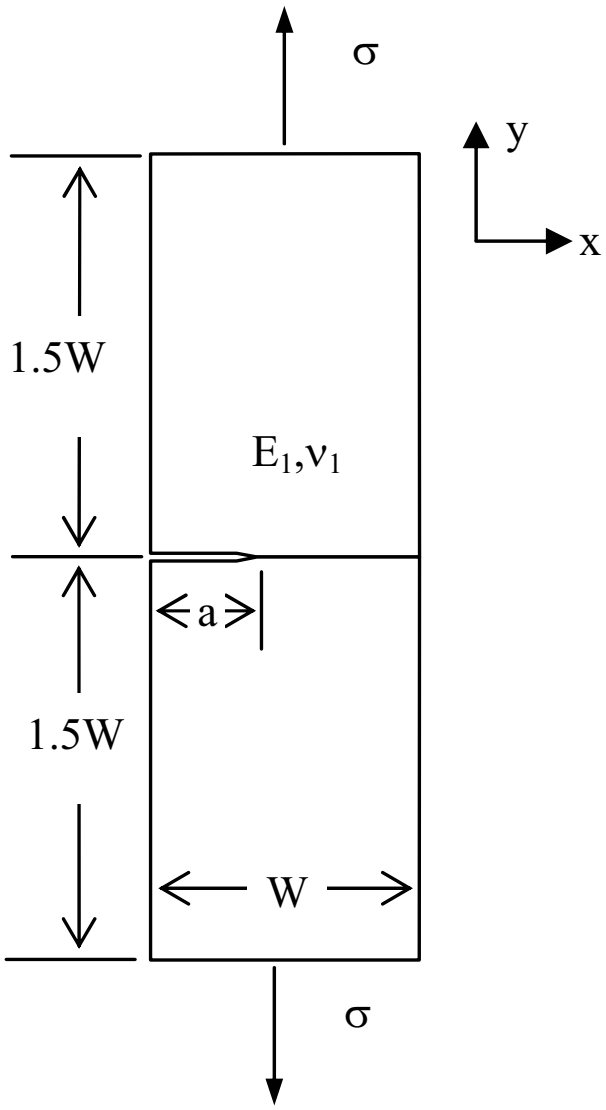

Figure 11 : Single edge interface crack

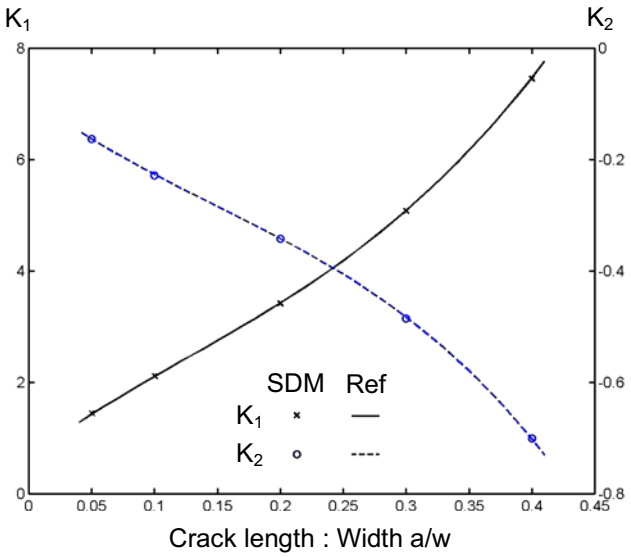

Figure 12a: K values for a/W – single edge interface crack (with E_1/E_2 = 2)

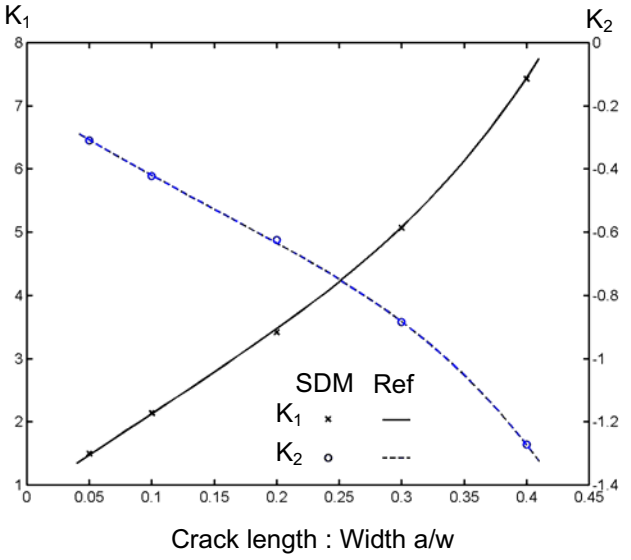

Figure 12b: K values for different a/W – single edge interface crack (with E_1/E_2 = 4)

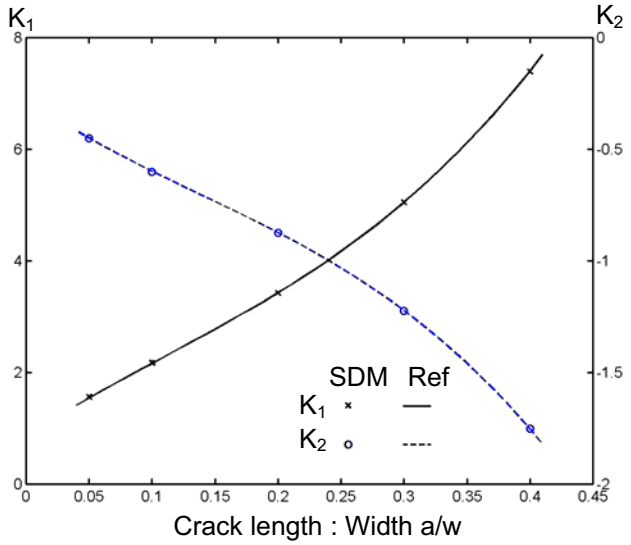

Figure 12c: K values for different a/W – single edge interface crack (with E_1/E_2 = 10)

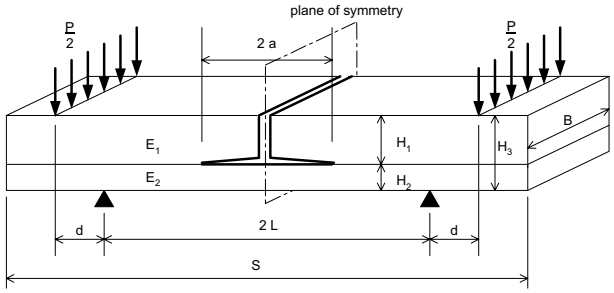

Figure 13: Four-point Bend Specimen

3.4 The Four-point Bend Specimen(Fig.13)

The following material and geometrical parameters are used: $E_1 = 3\times10^9$, $\nu_1 = \nu_2 = 0.3$

B=1, H_1 = 10B , S = 300B , d =H_3 ,

a = 45B , L = S/2 - $2H_3$

Reference values are taken from Charalambides, Lund, Evans and McMeeking (1989), in which graphical presentations of K are given in the normalized formats:

$$K_{1norm} = Re\left(KH_3^{i\varepsilon}\right)\frac{\cdot BH_3^{3/2}}{Pd}$$

and $$K_{2norm} = Im\left(KH_3^{i\varepsilon}\right)\frac{\cdot BH_3^{3/2}}{Pd}$$

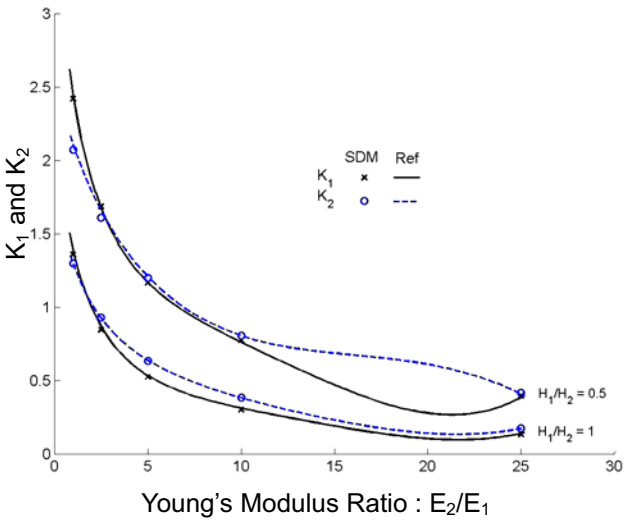

Figure 14: K values of different H_1/H_2 and E_1/E_2 ratios – four point bend specimen

Results calculated by the present approach are also converted to these forms for easy reference and are presented in Fig. 14. The maximum error is below 3.5%. It should be pointed out that the extraction of the normalized referenced values from the graphs in the reference makes it rather difficult to demonstrate extremely high accuracy.

4 Comparisons with other methods in accuracy

Several authors, namely, Wu (1994), Matos et al. (1989) and Chow et al. (1995), also analysed the infinite plate in Test Case 3.1 for validating complex stress intensity factors extraction techniques. Different material combinations were used for verification. Their reported percentage errors are shown in Tab. 1a-c. Our values for similar material combinations in Table 1d are obtained with e/a = 1/4 and m = 2.5, giving a coarse mesh of 166 elements. It can be seen that our accuracies are relatively high.

E_1/E_2	ν_1/ν_2	K_1 (%-error)	K_2 (%-error)
10	1	1.15	1.10
22	0.857	1.09	0.95
100	1	1.03	0.89

Table 1a: Accuracy in Matos et al. (1989) [160 elements]

E_1/E_2	ν_1/ν_2	K_1 (%-error)	K_2 (%-error)
10	1	1.16	1.04
22	0.857	1.07	1.115
100	1	0.99	1.03

Table 1b: Accuracy in Wu (1994) [160 elements]

E_1/E_2	ν_1/ν_2	K_1 (%-error)	K_2 (%-error)
5	1	1.18	0.70
50	1	1.01	0.00

Table 1c: Accuracy of Hybrid Element by Chow et al. (1995) [56 elements]

E_1/E_2	ν_1/ν_2	K_1 (%-error)	K_2 (%-error)
5	1	0.53	1.00
	0.857	0.52	0.98
	2.5	0.59	1.10
10	1	0.44	0.78
	0.857	0.43	0.75
	2.5	0.50	0.91
22	1	0.36	0.63
	0.857	0.35	0.60
	2.5	0.42	0.77
50	1	0.32	0.55
	0.857	0.30	0.51
	2.5	0.37	0.69
100	1	0.29	0.51
	0.857	0.28	0.47
	2.5	0.34	0.65

Table 1d: Accuracy of SDM [166 elements]

5 Applications to bimaterial anisotropic interfacial cracks

Basing primarily on the solutions of Qu and Bassani (1989, 1993), stress intensity factors for orthotropic plates have been studied by Chow and Atluri (1995) and Charalambides and Zhang (1996). In the former case the virtual crack closure integral method was employed and the procedure was also extended to anisotropic bimaterial continua in general. Using the expressions in Chow and Atluri (1995), the stress and displacement equations corresponding to equations (1) and (2) for orthotropic bimaterial media are:

$$\sqrt{\beta_2}\sigma_{22} + i\sqrt{\beta_1}\sigma_{12} = \frac{\sqrt{\beta_2}K_1 + i\sqrt{\beta_1}K_2}{\sqrt{2\pi r}} r^{i\varepsilon} \tag{18}$$

and

$$\sqrt{\beta_1}\delta_2 + i\sqrt{\beta_2}\delta_1$$

$$= \frac{(s_{\#1} - s_{\#2})\sqrt{2\pi r}\, r^{i\varepsilon}}{\pi\beta(1+2i\varepsilon)\cosh(\pi\varepsilon)} \left(\sqrt{\beta_2}K_1 + i\sqrt{\beta_1}K_2\right) \tag{19}$$

where β_1, β_2 , $s_{\#1}$ and $s_{\#2}$ are functions of stiffness coefficients while $\beta^2 = \beta_1\beta_2$. and equation (2) becomes

$$\varepsilon = \frac{1}{2\pi} \ln\left(\frac{1+\beta}{1-\beta}\right) \tag{20}$$

Relationships between stress intensity factors and strain energy release rates in equations (10) through (15) will also take more complicated forms.

In the case of anisotropic bimaterial continua in general, β has to be derived from operations on matrices of material constants, with correspondingly more complex forms for the stresses and displacements. A systematic listing of the relevant equations, both for the orthotropic and anisotropic cases can be found in Atluri (1997). These equations can be used to modify the expressions for the above stiffness-derivative-based procedure.

6 Conclusion

A method which integrates the stiffness derivative approach and a stress intensity factor perturbation procedure is presented. The stiffness derivative can be obtained in a finite-element analysis using crack-tip element nodal displacements and strain energies without the

generation of element stiffness matrices. Using a crack-tip element size to crack length ratio of 1/100, and a virtual crack extension to element size ratio of 1/500, accurate results can be obtained using relatively small number of elements.

Acknowledgement: The work described in this paper has been supported by the Research Grants Council of Hong Kong, China (Project no. PolyU 5512/98E) and the Hong Kong Polytechnic research fund G.43.37.T239.

References

Atluri, S. N. (1997): *Structural Integrity & Durability*, Tech Science Press, Forsyth, GA, 865 pages.

Charalambides, P. G.; Zhang, W. (1996): An energy method for calculating the stress intensities in orthotropic bimaterial fracture. *International Journal of Fracture*, vol. 76, pp. 97-120.

Charalambides, P. G.; Lund, J.; Evans, A. G.; McMeeking, R. M. (1989): A Test Specimen for Determining the Fracture Resistance of Bimaterials Interfaces. *Journal of Applied Mechanics*, vol. 56, pp. 77-82.

Chow, W. T.; Atluri, S. N. (1995): Finite element calculation of stress intensity factors for interfacial crack using virtual crack closure integral. *Computational Mechanics*, vol. 16, pp. 417-425.

Chow, W. T.; Atluri, S. N. (1996): Prediction of post-buckling strength of stiffened laminated composite panels based on the criterion of mixed-mode stress intensity factors. *Computational Mechanics*, v.18, pp.215-224.

Chow, W. T.; Beom, H. G.; Atluri, S. N. (1995): Calculation of stress intensity factors for an interfacial crack between dissimilar anisotropic media, using a hybrid element method and the mutual integral. *Computational Mechanics*, v.15, pp.15546-557.

Glaessgen, E. H.; Riddell, W. T.; Raju, I. S. (2002): Nodal constraint, shear deformation and continuity effects related to the modeling of debonding of laminates, using plate elements. *CMES: Computer Modeling in engineering & Sciences*, v.3, pp.103-116.

Hutchinson, J. W.; Suo, Z. (1992): Mixed mode cracking in layered materials. *Advances in Applied Mechanics*, v.29, pp.163-191.

Lin, K. Y.; Mar, J. W. (1976): Finite element analysis of stress intensity factors for cracks at bimaterial interface. *Internal Journal of Fracture*, vol. 12, pp. 521-531.

Matos, P. P. L.; McMeeking, R. M.; Charalambides, P. G.; Drory, M. D. (1989): A method for calculating stress intensities in bimaterial fracture, *International Journal of Fracture*, vol. 40, pp. 235-254.

Murakami, Y. (1987): *Stress intensity factors handbook*. The Society of Materials Science, Kyoto.

Naik, R. A.; Crews, J. H., Jr. (1994): Calculation of stress intensity factors for interface cracks under mixed-mode loading. *ASTM STP 1207*, pp.778-792.

Ng, S. W.; Lau, K. J. (2000): A new way of implementing the stiffness derivative method for determining stress intensity factors. *Internal Journal of Fracture*, vol. 102, pp. L29-L32.

Parks, D. M. (1974): A stiffness-derivative finite element technique for determination of elastic crack tip stress intensity factors. *International Journal of Fracture*, vol. 10, pp. 487-502.

Qu, J.; Bassani, J. L. (1993): Interfacial fracture mechanics for anisotropic bimaterials. *Journal of Applied Mechanics*. vol. 60, pp. 422-431.

Qu, J.; Bassani, J. L., (1989): Cracks on bimaterial and bicrystal interfaces. *Journal of the Mechanics and Physics of Solids*, vol. 37, pp. 417-433.

Williams, M. L. (1959), The stresses around a fault or crack in dissimilar media. *Bulletin of the Seismological Society of America*, vol. 49, pp. 199-204.

Wu, Y. L. (1994): A new method for evaluation of stress intensities for interface cracks. *Engineering Fracture Mechanics*, vol. 48, pp.755-761.

Appendix A: Functions f for asymptotic crack tip displacements

From Matos, KcMeeking, Charalambides and Drory (1989), the functions f_{x1}, f_{y1}, f_{x2} and f_{y2} are defined as follows (with reference to Fig. 1):

$f_{x1} = D_j + 2\delta_j \sin\theta \sin\psi$

$f_{y1} = -C_j - 2\delta_j \sin\theta \cos\psi$

$f_{x2} = -C_j + 2\delta_j \sin\theta \cos\psi$

$f_{y2} = -D_j + 2\delta_j \sin\theta \sin\psi$

where

$\delta_1 = e^{-(\pi-\theta)\varepsilon} \quad \delta_2 = e^{(\pi+\theta)\varepsilon}$

$\psi = \varepsilon \log r + \theta/2$

$$D_j = \beta\gamma_j \cos\tfrac{\theta}{2} + \beta'\gamma'_j \sin\tfrac{\theta}{2}$$

$$C_j = \beta'\gamma_j \cos\tfrac{\theta}{2} - \beta\gamma'_j \sin\tfrac{\theta}{2}$$

$$\beta = \frac{0.5\cos(\varepsilon \log r) + \varepsilon \sin(\varepsilon \log r)}{0.25 + \varepsilon^2}$$

$$\beta' = \frac{0.5\sin(\varepsilon \log r) - \varepsilon \cos(\varepsilon \log r)}{0.25 + \varepsilon^2}$$

$\gamma_j = \mu_j\delta_j - 1/\delta_j$, $\gamma'_j = \mu_j\delta_j + 1/\delta_j$